Title

Computational model of brain-stem circuit for state-dependent control of hypoglossal motoneurons

Journal

Journal of Neurophysiology, 120(7)

ISSN

0022-3077

Authors

Naji, Mohsen
Komarov, Maxim
Krishnan, Giri P
et al.

Publication Date

2018-07-01

DOI

10.1152/jn.00728.2017

Peer reviewed

J Neurophysiol 120: 296–305, 2018.
First published April 4, 2018; doi:10.1152/jn.00728.2017.

RESEARCH ARTICLE | *Neural Circuits*

Computational model of brain-stem circuit for state-dependent control of hypoglossal motoneurons

Mohsen Naji,[1] Maxim Komarov,[1] Giri P. Krishnan,[1] Atul Malhotra,[1] Frank L. Powell,[1] Irma Rukhadze,[2,3] Victor B. Fenik,[2,4] and Maxim Bazhenov[1]

[1]*Department of Medicine, Division of Pulmonary, Critical Care & Sleep Medicine, University of California, San Diego, La Jolla, California;* [2]*Veterans Affairs Greater Los Angeles Healthcare System, Los Angeles, California;* [3]*Department of Medicine, University of California, Los Angeles School of Medicine, Los Angeles, California; and* [4]*WebSciences International, Los Angeles, California*

Submitted 10 October 2017; accepted in final form 2 April 2018

Naji M, Komarov M, Krishnan GP, Malhotra A, Powell FL, Rukhadze I, Fenik VB, Bazhenov M. Computational model of brain-stem circuit for state-dependent control of hypoglossal motoneurons. *J Neurophysiol* 120: 296–305, 2018. First published April 4, 2018; doi:10.1152/jn.00728.2017.—In patients with obstructive sleep apnea (OSA), the pharyngeal muscles become relaxed during sleep, which leads to a partial or complete closure of upper airway. Experimental studies suggest that withdrawal of noradrenergic and serotonergic drives importantly contributes to depression of hypoglossal motoneurons and, therefore, may contribute to OSA pathophysiology; however, specific cellular and synaptic mechanisms remain unknown. In this new study, we developed a biophysical network model to test the hypothesis that, to explain experimental observations, the neuronal network for monoaminergic control of excitability of hypoglossal motoneurons needs to include excitatory and inhibitory perihypoglossal interneurons that mediate noradrenergic and serotonergic drives to hypoglossal motoneurons. In the model, the state-dependent activation of the hypoglossal motoneurons was in qualitative agreement with in vivo data during simulated rapid eye movement (REM) and non-REM sleep. The model was applied to test the mechanisms of action of noradrenergic and serotonergic drugs during REM sleep as observed in vivo. We conclude that the proposed minimal neuronal circuit is sufficient to explain in vivo data and supports the hypothesis that perihypoglossal interneurons may mediate state-dependent monoaminergic drive to hypoglossal motoneurons. The population of the hypothesized perihypoglossal interneurons may serve as novel targets for pharmacological treatment of OSA.

NEW & NOTEWORTHY In vivo studies suggest that during rapid eye movement sleep, withdrawal of noradrenergic and serotonergic drives critically contributes to depression of hypoglossal motoneurons (HMs), which innervate the tongue muscles. By means of a biophysical model, which is consistent with a broad range of empirical data, we demonstrate that the neuronal network controlling the excitability of HMs needs to include excitatory and inhibitory interneurons that mediate noradrenergic and serotonergic drives to HMs.

biophysical model; hypoglossal motoneurons; noradrenaline; obstructive sleep apnea; serotonin

Address for reprint requests and other correspondence: M. Bazhenov, 9500 Gilman Dr., MC-7381, La Jolla, CA 92093-7381 (e-mail: mbazhenov@ucsd.edu).

INTRODUCTION

Dynamic neuromuscular control of the upper airway dilator muscles differs during wakefulness and sleep. Suppression of activity in these muscles causes repetitive partial or complete obstruction of upper airway in patients with obstructive sleep apnea (OSA) whose upper airways commonly have anatomic features that reduce the size of airway orifice (Horner et al. 1989; Remmers et al. 1978). During wakefulness, a neuromuscular compensation overcomes these anatomic deficiencies and maintains patency of upper airway allowing patients with OSA to breathe (Mezzanotte et al. 1992). However, this compensation is lost at sleep onset via sleep-related depressant mechanisms that cause relaxation of the pharyngeal muscles leading to obstructive events during sleep (Suratt et al. 1988). The upper airway muscle tone and the airway patency is further reduced during rapid eye movement (REM) sleep, which is consistent with the increased severity of obstruction episodes during REM sleep (Eckert et al. 2009; Trinder et al. 2014). The neurochemical control of pharyngeal muscles during wakefulness and sleep is not well understood.

The activity of hypoglossal motoneurons that innervate tongue and pharyngeal muscles, including the genioglossus, are essential for maintaining upper airway patency, especially in those who are anatomically compromised. Methods including electrical stimulation of hypoglossal nerve (Malhotra 2014; Schwartz et al. 2014; Strollo et al. 2014) as well as chemostimulation (Pillar et al. 2000) and pharmacological interventions (Chan et al. 2006; Fenik et al. 2004, 2005a, 2005b; Fleury Curado et al. 2017; Grace et al. 2013; Horton et al. 2017; Morrison et al. 2003; Sood et al. 2005; Steenland et al. 2006) have been applied to hypoglossal motoneurons to maintain pharyngeal patency. Understanding of neurological mechanisms of sleep-related changes in neurochemical drive to hypoglossal motoneurons may help developing pharmaceutical treatment for OSA (Jordan et al. 2014).

At present, there is no consensus regarding the exact mechanisms responsible for REM sleep-related depression of hypoglossal motoneurons (REM-HD; Bellingham and Berger 1996; Chan et al. 2006; Fenik et al. 2004, 2005a, 2005b, 2015; Fung and Chase 2015; Grace et al. 2013; Kodama et al. 2003; Kubin et al. 1992, 1993; Lai et al. 2001; Lydic 2008; Morrison et al.

2003; Parkis et al. 1995; Sood et al. 2005; Steenland et al. 2006; Yamuy et al. 1999). Multiple neurotransmitters have been suggested to play a role in the control of hypoglossal motoneurons during REM sleep: glycine (Fung and Chase 2015; Kodama et al. 2003; Yamuy et al. 1999), GABA (Kodama et al. 2003), serotonin (5-HT; Fenik et al. 2005b; Kubin et al. 1992; Lai et al. 2001), noradrenaline (NA; Chan et al. 2006; Fenik et al. 2005b; Lai et al. 2001; Yamuy et al. 1999), glutamate (Bellingham and Berger 1996), and acetylcholine (ACh; Bellingham and Berger 1996; Grace et al. 2013). However, the most conclusive results were obtained in studies in which application of receptor antagonists that target glycine, $GABA_A$, 5-HT, and α_1-adrenergic receptors into the hypoglossal nucleus abolished REM-HD during carbachol-induced REM sleep-like state in anesthetized rats (Fenik et al. 2004). Follow-up experiments revealed that antagonizing α_1-adrenoceptors and 5-HT receptors was necessary and sufficient to abolish REM-HD (Fenik et al. 2005b). Importantly, similar findings were obtained in a series of studies conducted in chronically implanted behaving rats, which were designed to test the role of glycinergic, GABAergic, 5-HT, and NA transmission in depression of genioglossus muscle activity during REM sleep in behaving rats (Chan et al. 2006; Morrison et al. 2003; Sood et al. 2005).

Since REM-HD was abolished with a considerable delay of 30–60 min following injection of the antagonists into the hypoglossal nucleus (Fenik et al. 2004, 2005a, 2005b), it was proposed that the antagonists had to diffuse outside of the hypoglossal nucleus to block receptors, which are located on interneurons mediating the aminergic drive to hypoglossal motoneurons (HM; Fenik et al. 2005a). Additional analysis of the antagonist effects and their time courses allowed developing a hypothetical brain-stem neuronal network that controls the state-dependent excitability of HM (Fenik 2015). The key elements of this network were pontine noradrenergic A7 and medullary raphe 5-HT neurons that are REM-OFF neurons (Fenik et al. 2015; Heym et al. 1982; Rukhadze et al. 2008; Trulson and Jacobs 1979) and the hypothetical excitatory and inhibitory interneurons that are likely to be located in perihypoglossal region and mediate noradrenergic and 5-HT drives to HMs (Fenik 2015). In this study, we developed a computational network model to test this hypothesis and to investigate the impact of withdrawal of noradrenergic and serotonergic drives during the transition from non-REM (NREM) sleep to REM sleep on HM activity.

MATERIALS AND METHODS

Biophysical Model

The HMs have a linear frequency input-current relationship as shown in experiments (Sawczuk et al. 1995), which was also replicated by a detailed ionic model of HM neurons (Purvis and Butera 2005). Thus we assumed that activity of HMs is related to the excitatory drive from excitatory perihypoglossal interneurons (EPI) through a linear transformation. To model activity of EPI, we considered a network model that contained 4 neuronal populations: A7 noradrenergic neurons, 5-HT neurons in raphe nuclei, inhibitory perihypoglossal interneurons (IPI; which are likely to be GABAergic), and EPI, connected to each other as shown in Fig. 2*A*. All of the neuronal populations contained 500 neurons in these model simulations.

Models for Individual Neuron Dynamics

The populations of the IPI and EPI were modeled using Hodgkin-Huxley formalism. Since there are no direct recordings from IPI and EPI, we used a canonical model of spiking neuron with spike frequency adaptation (Colbert and Pan 2002; Mainen and Sejnowski 1996; Traub 1982). The membrane potential of each neuron was governed by the following equation (Komarov and Bazhenov 2016):

$$C_{\mathrm{m}}\frac{\mathrm{d}V}{\mathrm{d}t} = -I_{\mathrm{Na}} - I_{\mathrm{K}} - I_{\mathrm{KCa}} - I_{\mathrm{Ca}} - I_{\mathrm{syn}} - I_{\mathrm{Leak}} - \eta\xi_i,$$

where V represents transmembrane voltage of the neuron, C_{m} stands for membrane capacitance, I_{Na} is fast Na^+ current (Colbert and Pan 2002; Traub 1982), I_{K} is a delayed rectifier K^+ current (Traub 1982), I_{KCa} is slow Ca^{2+}-dependent K^+ current (Mainen and Sejnowski 1996), I_{Ca} is a high-threshold-activated Ca^{2+} current (Mainen and Sejnowski 1996), I_{syn} is synaptic current, I_{Leak} is a leak current, and the term $\eta\xi_i(t)$ corresponds to the fluctuations in the transmembrane current (representing spontaneous background activity), which are given by a white noise process with the following properties: $<\xi_i(t)> = 0$, $<\xi_i(t)\xi_i(t - t_0)> = \delta(t - t_0)$. Following a common practice (Cressman et al. 2009; Destexhe et al. 2001; Krishnan et al. 2015), we assumed in the model that the I_{Leak} represents the effects of Na^+, K^+, and Cl^- leak currents, with predominant contribution of the K^+ leak. Each ionic current was modeled using Hodgkin-Huxley formalism:

$$I_{\mathrm{Na}} = g_{\mathrm{Na}}m^3h(V - E_{\mathrm{Na}})$$
$$I_{\mathrm{K}} = g_{\mathrm{K}}n^4(V - E_{\mathrm{K}})$$
$$I_{\mathrm{KCa}} = g_{\mathrm{KCa}}m_{\mathrm{KCa}}(V - E_{\mathrm{K}})$$
$$I_{\mathrm{Ca}} = g_{\mathrm{Ca}}m_{\mathrm{Ca}}^2h_{\mathrm{Ca}}(V - E_{\mathrm{Ca}}),$$

where g_x is a maximal conductance, E_x is a reversal potential, n describes the activation of potassium current, and m_x and h_x are activation and inactivation gating variables, correspondingly [subscript x denotes 1 of the ionic currents $x \in$ (Na, K, KCa, Ca)]. The gating variables obey the following equation:

$$\tau_y(V)\frac{\mathrm{d}y}{\mathrm{d}t} = y_\infty(V) - y,$$

where y is 1 of the gating variables, and voltage-dependent functions $y_\infty(V)$ and $\tau_y(V)$ are:

$$m_\infty(V) = \frac{\alpha_m(V)}{\alpha_m(V) + \beta_m(V)},\ \tau_m(V) = \frac{1}{\varphi[\alpha_m(V) + \beta_m(V)]}$$

$$\alpha_m(V) = \frac{0.182(V + 38)}{1 - \exp[-(V + 38)/6]},\ \beta_m(V) = \frac{-0.124(V + 38)}{1 - \exp[(V + 38)/6]}$$

$$h_\infty(V) = \frac{\alpha_h(V)}{\alpha_h(V) + \beta_h(V)},\ \tau_h(V) = \frac{1}{\varphi[\alpha_h(V) + \beta_h(V)]}$$

$$\alpha_h(V) = \frac{-0.015(V + 66)}{1 - \exp[(V + 66)/6]},\ \beta_h(V) = \frac{0.015(V + 66)}{1 - \exp[-(V + 66)/6]}$$

$$n_\infty(V) = \frac{\alpha_n(V)}{\alpha_n(V) + \beta_n(V)},\ \tau_n = 1.8\ \mathrm{ms}$$

$$\alpha_n(V) = \frac{0.0035(V + 30)}{1 - \exp[-(V + 30)/13]},\ \beta_n(V) = \frac{-0.0035(V + 30)}{1 - \exp[(V + 30)/13]}$$

$$m_\infty^{\mathrm{Ca}} = \frac{\alpha_m^{\mathrm{Ca}}(V)}{\alpha_m^{\mathrm{Ca}}(V) + \beta_m^{\mathrm{Ca}}(V)},\ \tau_m^{\mathrm{Ca}} = \frac{1}{\varphi[\alpha_m^{\mathrm{Ca}}(V) + \beta_m^{\mathrm{Ca}}(V)]}$$

$$\alpha_m^{\mathrm{Ca}} = \frac{0.055(27 + V)}{1 - \exp[-(27 + V)/3.8)]},\ \beta_m^{\mathrm{Ca}} = \frac{0.94}{1 + \exp[-(75 + V)/17]}$$

$$h_\infty^{\mathrm{Ca}} = \frac{\alpha_h^{\mathrm{Ca}}(V)}{\alpha_h^{\mathrm{Ca}}(V) + \beta_h^{\mathrm{Ca}}(V)},\ \tau_h^{\mathrm{Ca}} = \frac{1}{\varphi[\alpha_h^{\mathrm{Ca}}(V) + \beta_h^{\mathrm{Ca}}(V)]}$$

$$\alpha_h^{\mathrm{Ca}} = 0.00457\exp[-(13+V)/50],\ \beta_h^{\mathrm{Ca}} = \frac{0.0065}{1+\exp[-(15+V)/28]}$$

$$m_\infty^{\mathrm{KCa}} = \frac{\alpha_m^{\mathrm{KCa}}([\mathrm{Ca}^{2+}])}{\alpha_m^{\mathrm{KCa}}([\mathrm{Ca}^{2+}]) + \beta_m^{\mathrm{KCa}}(V)},\ \tau_m^{\mathrm{KCa}} = \frac{1}{\varphi[\alpha_m^{\mathrm{KCa}}([\mathrm{Ca}^{2+}]) + \beta_m^{\mathrm{KCa}}(V)]}$$

$$\alpha_m^{\mathrm{KCa}} = 0.01[\mathrm{Ca}^{2+}],\ \beta_m^{\mathrm{KCa}} = 0.02,\ \text{temperature factor } (\varphi) = 3.488.$$

The functions $\alpha(V)$, $\beta(V)$, and $\tau(V)$ have dimensions of per millisecond, per millisecond, and milliseconds.

Dynamics of calcium concentration ($[\mathrm{Ca}^{2+}]$) obey the following equation:

$$\frac{\mathrm{d}[\mathrm{Ca}^{2+}]}{\mathrm{d}t} = -\gamma I_{\mathrm{Ca}} + ([\mathrm{Ca}^{2+}]_\infty - [\mathrm{Ca}^{2+}])/\tau_{\mathrm{Ca}}.$$

The leak current consists of two parts: $I_{\mathrm{Leak}} = I_{\mathrm{K}} + I_{\mathrm{l}}$, where $I_{\mathrm{l}} = g_{\mathrm{l}}(V - E_{\mathrm{l}})$ is a generic leak current, and $I_{\mathrm{K}}^{\mathrm{Leak}} = g_{\mathrm{K}}^{\mathrm{Leak}}(V - E_{\mathrm{K}})$ is a potassium leak current (Bazhenov et al. 2002). A full list of parameters is given at the end of MATERIALS AND METHODS.

Spiking activity of populations of A7 and raphe neurons was modeled using Poisson process, in which the characteristic frequency (λ) depended on the sleep stage. The spike times (t_i) were iteratively generated from the formula $t_{i+1} = t_i - \log(x)/\lambda$, where x is uniformly distributed between 0 and 1.

For each spike in the A7 and raphe neuron populations, the transmitter is assumed to be released according to a 3-ms pulse with amplitude 1 (Destexhe et al. 1994). Then, the average [NA] and [5-HT] concentrations are calculated across neurons in EPI and IPI populations, respectively. In summary, the transmitter concentration ([T]) is calculated as follows:

$$[\mathrm{T}] = \frac{1}{N}\sum_{i=1}^{N} P_i(t),\ P_i(t) = \begin{cases} 1\ t_{\mathrm{spike}}(j) < t < t_{\mathrm{spike}}(j) + 3\ \mathrm{ms} \\ 0\ \text{otherwise} \end{cases},$$
$$j = 1, ..., N_{\mathrm{s}},$$

where $P_i(t)$ is time series of 3-ms pulses for the ith neuron, and N_{s} is the number of spikes.

Models for Action Of Neuromodulators (5-HT and NA) and Drugs (Methysergide and Prazosin)

Prazosin (Pz) is an inverse agonist of α-adrenergic receptors (Rossier et al. 1999), which on binding to receptor blocks the receptor, whereas methysergide (Me) is proposed to behave as a partial agonist of $5\text{-HT}_{1\mathrm{A}}$ receptor (Colpaert et al. 1979), which is reflected in facilitating the transition from closed to open states. Therefore, we used different transition kinetic schemes to describe the pharmacological antagonism by Pz and Me.

Interneurons. The scheme presented in Fig. 2*A* assumes that each neuron in the population of IPI contains serotonergic 5-HT receptors, which are able to produce cell inhibition through opening of K^+ channels. The dynamics of 5-HT receptors under action of 5-HT and Me were modeled based on the following transition scheme (Destexhe et al. 1994):

$$[\mathrm{O}] \underset{\alpha = K_1([5\text{-HT}]+[\mathrm{Me}])}{\overset{\beta}{\rightleftharpoons}} [\mathrm{C}].$$

Here, labels [O] and [C] denote opened and closed state of the 5-HT receptor, correspondingly, and α and β denote rates of transition between the states. The rate of transition from closed to open state is a linear function of the sum of 5-HT and Me concentrations, $\alpha = K_1([5\text{-HT}] + [\mathrm{Me}])$. The rate of transition from opened to the closed state is constant (β). The scheme described above leads to the following first-order kinetic equation for the fraction of the opened serotonergic receptors:

$$\frac{\mathrm{d}r}{\mathrm{d}t} = K_1([5\text{-HT}] + [\mathrm{Me}])(1 - r) - \beta_{\mathrm{IPI}} r,$$

which, in turn, produce activation of intracellular G protein (G):

$$\frac{\mathrm{d}[\mathrm{G}]}{\mathrm{d}t} = K_{2\mathrm{IPI}} r - K_{3\mathrm{IPI}}[\mathrm{G}].$$

Finally, activation of G protein modulates potassium leak current in the following way:

$$I_{\mathrm{K}}^{\mathrm{Leak}} = g_{\mathrm{K}} \frac{[\mathrm{G}]^4}{[\mathrm{G}]^4 + K_{\mathrm{dIPI}}}(V - E_{\mathrm{K}}).$$

The scheme presented in Fig. 2*B* assumes that each neuron in population of EPI interneurons contains α_1-adrenergic receptors, for which activation can facilitate cell activation. The dynamics of NA receptors under action of noradrenaline and prazosin (Pz) were modeled based on the following transition scheme:

$$[\mathrm{O}] \underset{\alpha = K_4[\mathrm{NA}]}{\overset{\beta}{\rightleftharpoons}} [\mathrm{C}] \underset{\delta}{\overset{\gamma = K_5[\mathrm{Pz}]}{\rightleftharpoons}} [\mathrm{B}].$$

Here, [O], [C], and [B] denote opened, closed, and blocked state, correspondingly. NA and Pz compete for the noradrenergic receptors, transforming them to either opened (NA) or blocked (Pz) states. The rate of transition of closed to opened state depends on the concentration of NA: $\alpha = K_4[\mathrm{NA}]$, whereas transition from closed to blocked state is controlled by concentration of Pz: $\gamma = K_5[\mathrm{Pz}]$. $K_{4,5}$ are positive constants. The scheme described above leads to the following equations for fraction of opened (O), closed (C), and blocked (B) receptors, where $\dot{P}$ is derivative of P:

$$\begin{cases} \dot{P_{\mathrm{O}}} = \alpha P_{\mathrm{C}} - \beta P_{\mathrm{O}} \\ \dot{P_{\mathrm{C}}} = \beta P_{\mathrm{O}} + \delta P_{\mathrm{B}} - \gamma P_{\mathrm{C}} - \alpha P_{\mathrm{C}} \\ \dot{P_{\mathrm{B}}} = \gamma P_{\mathrm{C}} - \delta P_{\mathrm{B}} \\ P_{\mathrm{O}} + P_{\mathrm{B}} + P_{\mathrm{C}} = 1 \end{cases}.$$

Similar to the case of IPI, opening of NA receptors leads to activation of the second messenger (S) and modulation of K^+ currents:

$$\frac{\mathrm{d}[\mathrm{S}]}{\mathrm{d}t} = K_{2\mathrm{EPI}} P_{\mathrm{O}} - K_{3\mathrm{EPI}}[\mathrm{S}]$$

$$I_{\mathrm{K}}^{\mathrm{Leak}} = \bar{g}_{\mathrm{K}}\left(1 - \frac{[\mathrm{S}]^4}{[\mathrm{S}]^4 + K_{\mathrm{dEPI}}}\right)(V - E_{\mathrm{K}}).$$

Each model neuron in the IPI and EPI populations implements the leak current-simulating effects of activation of 5-HT and NA receptors, respectively. Each model neuron in the EPI population also incorporates synaptic currents from all of the IPI GABAergic neurons.

Postsynaptic I_{syn} for the EPI inhibitory synapses were defined by standard $\mathrm{GABA_A}$ receptor model (Destexhe et al. 1998), which is described by first-order kinetics:

$$I_{\mathrm{syn}} = \bar{g}_{\mathrm{GABA_A}} s(t)(V - E_{\mathrm{GABA_A}}).$$

Gating variable $s(t)$ is governed by the following equation:

$$\frac{\mathrm{d}s}{\mathrm{d}t} = \alpha_s[\mathrm{T}](1 - s) - \beta_s s.$$

The $\mathrm{GABA_A}$ transmitter (T) is assumed to be 1 for 1 ms when an action potential invades the presynaptic terminal and 0 otherwise.

Parameters. PARAMETERS FOR IPI. $C_{\mathrm{m}} = 1\ \mu\mathrm{F/cm^2}$, $E_{\mathrm{Na}} = 55$ mV, $E_{\mathrm{K}} = -85$ mV, $E_{\mathrm{l}} = -71$ mV, $E_{\mathrm{Ca}} = 120$ mV, $g_{\mathrm{Na}} = 150\ \mathrm{mS/cm^2}$, $g_{\mathrm{K}} = 10\ \mathrm{mS/cm^2}$, $g_{\mathrm{KCa}} = g_{\mathrm{Ca}} = 0\ \mathrm{mS/cm^2}$, $g_{\mathrm{l}} = 0.015\ \mathrm{mS/cm^2}$,

$\tau_{Ca} = 400$ ms, $[Ca^{2+}]_\infty = 2.4 \times 10^{-4}$ mM, $\beta_{IPI} = 5$, $K_1 = 1$, $K_{2IPI} = 0.18$, $K_{3IPI} = 0.034$, and $K_{dIPI} = 250$.

PARAMETERS FOR EPI. $C_m = 1$ μF/cm^2, $E_{Na} = 55$ mV, $E_K = -85$ mV, $E_l = -71$ mV, $E_{Ca} = 120$ mV, $E_{GABA_A} = -80$ mV, $g_{Na} = 75$ mS/cm^2, $g_K = 25$ mS/cm^2, $g_{KCa} = 1.5$ mS/cm^2, $g_{Ca} = 0.2$ mS/cm^2, $g_l = 0.022$ mS/cm^2, $g_{GABA_A} = 0.04$ μS, $\tau_{Ca} = 400$ ms, $[Ca^{2+}]_\infty = 2.4 \times 10^{-4}$ mM, $\beta_{EPI} = 5$, $\delta_{EPI} = 5$, $K_{2EPI} = 0.18$, $K_{3EPI} = 0.034$, $K_{4,5} = 1$, $K_{dEPI} = 5$, $\alpha_s = 0.25$, and $\beta_s = 0.05$.

Simulations and Data Analysis

The model was implemented in C++. In numerical simulations of the described model (10 simulations, 40 s each), we used the 4th-order Runge-Kutta method with constant time step 0.01 ms. Spike timing in neurons was detected when the neuron membrane voltage crossed a voltage threshold (−20 mV) and the time from previous spike was >4 ms.

RESULTS

Pharmacological Interventions Reveal Interactions between Brain-Stem Nuclei in the Hypoglossal Motoneurons Control

A conceptual model of a brain-stem neural network that can potentially explain in vivo data on state-dependent control of hypoglossal motoneurons has been proposed in Fenik (2015). In this model, the main neuronal populations that are responsible for the state-dependent control of hypoglossal motoneurons (HMs) include 5 distinct populations of cells [Fig. 1*A*, from Fenik (2015)]: 5-HT raphe neurons (RN), noradrenergic A7 neurons, local inhibitory possibly GABAergic interneurons, excitatory interneurons [reticular formation neurons (RF-neurons)], and HMs. HMs are indirectly controlled by A7 neurons through the populations of RF-neurons. The RN provided inhibitory 5-HT projections to the inhibitory interneurons that, in turn, inhibit the RF-neurons. In vivo data behind this conceptual model are summarized below.

Recordings from 18 presumed 5-HT neurons within nucleus raphe pallidus in freely moving cats showed the highest activity during wakefulness (mean: 4.85 ± 0.37 spikes/s) with gradually reduced activity during NREM sleep (mean: 3.76 ± 0.36 spikes/s) and the least activity during REM sleep (mean: 0.92 ± 0.23 spikes/s; Heym et al. 1982). We also previously obtained preliminary data from 6 putative noradrenergic A7 neurons in naturally sleeping head-restrained rats, which had tonic low-frequency discharges during wakefulness (mean: 1.20 ± 0.19 spikes/s) and NREM sleep (mean: 0.97 ± 0.4 spikes/s) and were almost silent (mean: 0.092 ± 0.09 spikes/s)

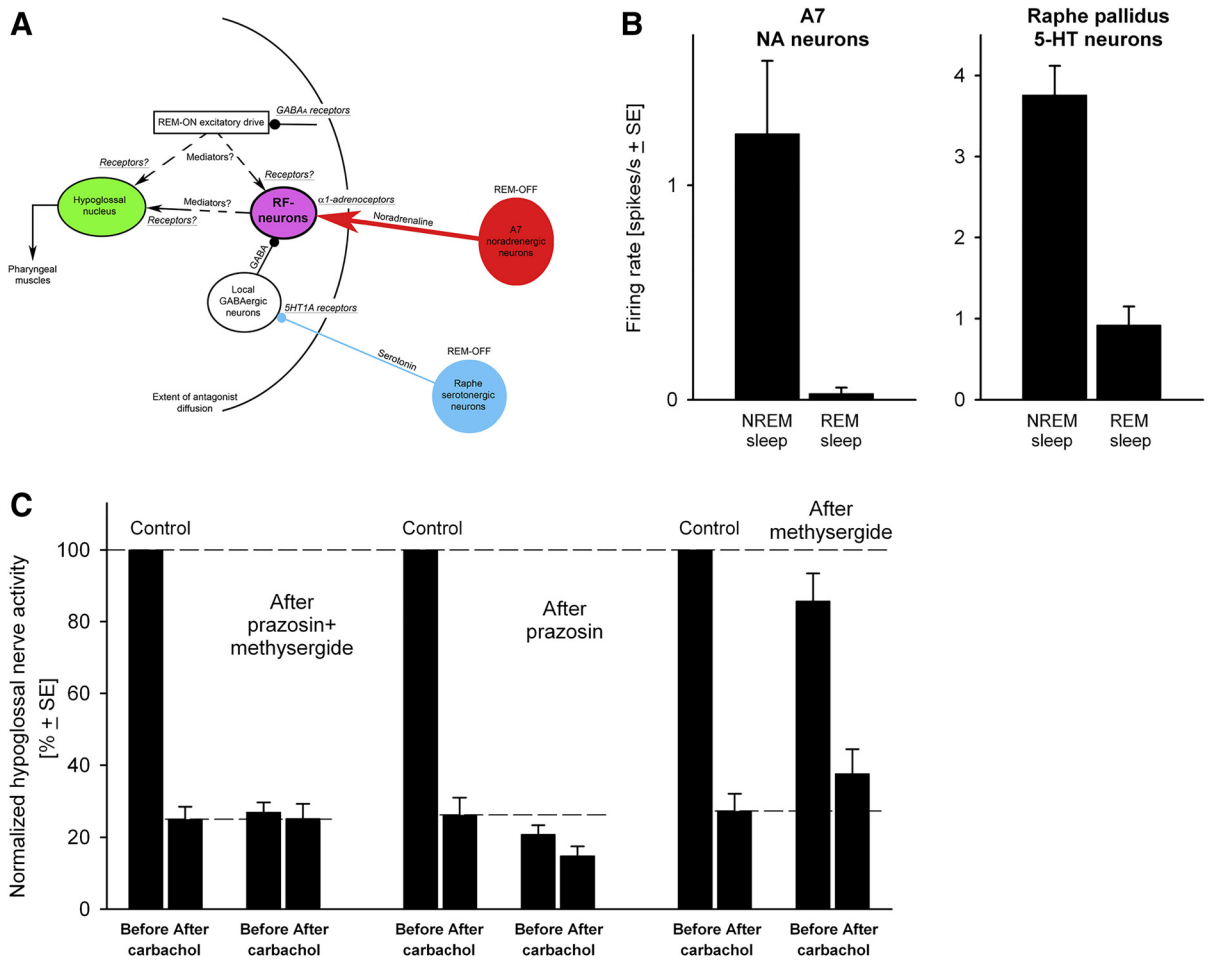

Fig. 1. Empirical data that were used to construct and validate the biophysical model of a network to provide monoaminergic control of hypoglossal motoneuronal (HM) activity. *A*: a brain-stem circuit that illustrates the main neural populations responsible for state-dependent control of HM [from Fenik (2015)]. RF-neurons, reticular formation neurons. *B*: recordings from A7 noradrenergic (NA) neurons (Fenik et al. 2015) and raphe neurons (Heym et al. 1982) revealed that they have lower activity during rapid eye movement (REM) compared with non-REM (NREM) sleep. *C*: hypoglossal nerve activities during carbachol-induced REM sleep-like episodes that were evoked before and after the injection of methysergide, prazosin, or a mixture of prazosin and methysergide.

during REM sleep. One-way ANOVA resulted in $F_{5,2} = 9.15$, $P < 0.01$, and significant differences ($P < 0.05$) between REM and NREM sleeps as well as between REM sleep and wakefulness (Bonferroni pairwise comparison; Fenik et al. 2015). Figure 1*B* summarizes mean activity of A7 and raphe pallidus neurons during NREM and REM sleep.

The injection of a solution of prazosin (Pz) and methysergide (Me) into the hypoglossal nucleus abolished REM sleep-related depression of HMs (REM-HD) that was induced by pontine injection of carbachol in anesthetized rats (Fenik et al. 2005b). These findings are summarized in Fig. 1*C* [values from Fenik et al. (2005b)]. Following 27–83 min after the combined antagonist injections, hypoglossal nerve activity was disfacilitated to 27.0% of baseline, approximately the level measured during control carbachol responses, and carbachol injected at this time period was unable to reduce activity in hypoglossal nerve further.

Two other separated trials with injections of "prazosin only" and "methysergide only" were conducted to quantify the contribution of noradrenergic and serotonergic neurotransmission to REM-HD. Following the prazosin only injections, the HM activity was reduced to 20.8% of baseline, below the control carbachol level (26.1%), and further reduced by another carbachol injection to 14.8%. Thus, despite the fact that HM activity was reduced by prazosin more than by the mixture of prazosin and methysergide, the reduced activities before and after carbachol injection had a significant difference revealing a remaining REM-HD of ~6%. Using these numbers, we can calculate the relative contribution of 5-HT and NA mechanisms to REM-HD as the following: the estimated relative contribution of serotonergic mechanisms to REM-HD is $(20.8 - 14.8)/(100 - 14.8) = 7\%$, and the relative contribution of noradrenergic mechanism is $(100 - 20.8)/(100 - 14.8) = 93\%$ (see also Fenik 2015).

After the methysergide only injections, the HM activity was reduced only to 85.8% of baseline, and carbachol injections elicited a strong REM-HD. Note that following methysergide, the HM activity after carbachol administration was significantly higher (37.6%) than during the control REM sleep-like state before the antagonists (27.2% on baseline activity), suggesting a disinhibitory effect of methysergide on REM-HD (Fenik et al. 2005b).

Collectively, these data suggest that prazosin may be fully responsible for the disfacilitation and methysergide for disinhibitory effect on REM-HD.

Based on the physiological data described above, we designed a biophysical model representing dynamics of the main neuronal groups within the network responsible for the state-dependent control of HM and predicted changes in their behavior under different physiological conditions, such as during NREM and REM sleep, and under different concentrations of Pz and Me.

Biophysical Model

We designed a biophysical model to explore the role of proposed neuronal populations and neurotransmitters in state-dependent control of HMs (Fig. 2*A*). We assumed that the activity of HMs was linearly related to that of the excitatory perihypoglossal interneurons (EPI). This excitatory drive from EPI to HMs depended on the interactions among four distinct neuronal populations: A7 neurons, 5-HT RN, EPI, and inhibitory perihypoglossal interneurons (IPI).

Baseline model. We set firing of A7 neurons and RN in the model to be equal to those obtained in in vivo experimental recordings during NREM and REM sleep for A7 (1.03 ± 0.16 and 0.15 ± 0.09 Hz, respectively) and RN (3.79 ± 0.31 and 0.93 ± 0.15 Hz, respectively; Fig. 2, *B* and *C*). The reduction of the firing rate of REM-OFF A7 neurons and RN during the transition from NREM to REM sleep decreases the release of NA and 5-HT neurotransmitters.

The status of α_1-adrenoceptors in EPI and 5-HT_{1A} receptors in IPI determined the state of potassium leak currents in these neurons. We assumed that the EPI also received GABAergic inhibitory drive from the IPI that affected the postsynaptic currents of the EPI. Figure 2, *D* and *E*, shows the activity of the IPI and EPI populations during NREM and REM sleep stages in the model. Relatively high activity of RN during NREM sleep inhibited activity of IPI compared with REM sleep (Fig. 2*D*). The net effect of reduced excitatory drive from A7 neurons and increased inhibitory drive from IPI resulted in a markedly lower activity of EPI during REM sleep compared with NREM sleep (Fig. 2, *E* and *F*), which was in line with experimental recordings from HMs (Fig. 1*C*). Thus the behavior of EPI in the baseline model was REM-OFF and mimicked the activity of HMs during NREM and REM sleep, whereas the behavior of IPI had the REM-ON pattern, i.e., they were more active during REM sleep compared with NREM sleep.

Effects of prazosin and methysergide on the neural behavior in the basic model. Starting from the baseline model, we studied the effect of different extracellular concentrations of Pz, an α_1-adrenergic antagonist, and Me. Me is a broad-spectrum 5-HT antagonist. In our model, it worked as an agonist of inhibitory 5-HT_{1A} receptors as proposed previously (Scrogin et al. 2000; Trulson and Jacobs 1979). The levels of the concentration of Pz and NA in the model varied within a broad range of values that competed to affect the probability of α_1-adrenoceptors located on the EPI to be in the open or closed states (Fig. 3, *A* and *C*). An increase in the Pz level and a decrease of the NA drive resulted in the reduction of the probability of α_1-adrenoceptors to be open (Fig. 3*C*). Conversely, Me worked as an agonist and helped 5-HT to increase the probability of the 5-HT_{1A} serotonergic receptor of the IPI to be in the open state (Fig. 3, *B* and *D*).

Figure 4, *A* and *B*, illustrates the effect of different levels of Pz and Me on the firing rate of EPI during NREM and REM sleep. In both cases, increasing the prazosin level decreased the EPI activity, whereas increasing methysergide level slightly increased the EPI activity. The effect of the prazosin was most prominent during NREM sleep, which is illustrated by plotting EPI firing vs. Pz level (see *inset* in Fig. 4*A*). Thus the model explained the effect of competition between prazosin and methysergide in controlling activity of the EPI population. Next, we selected the values for Pz and Me to match model responses to the empirical data of the application of the agonists across sleep stages (Fig. 1). Existence of the match supports our hypothesis that proposed network circuit (Fig. 2*A*) is sufficient to explain EPI (and therefore HM) behavior under control conditions and following drug applications.

The results of the model behavior are summarized in Fig. 4, *C–F*. The antagonists, Pz and Me, affected receptors that are located on EPI and IPI, respectively. Therefore, they changed

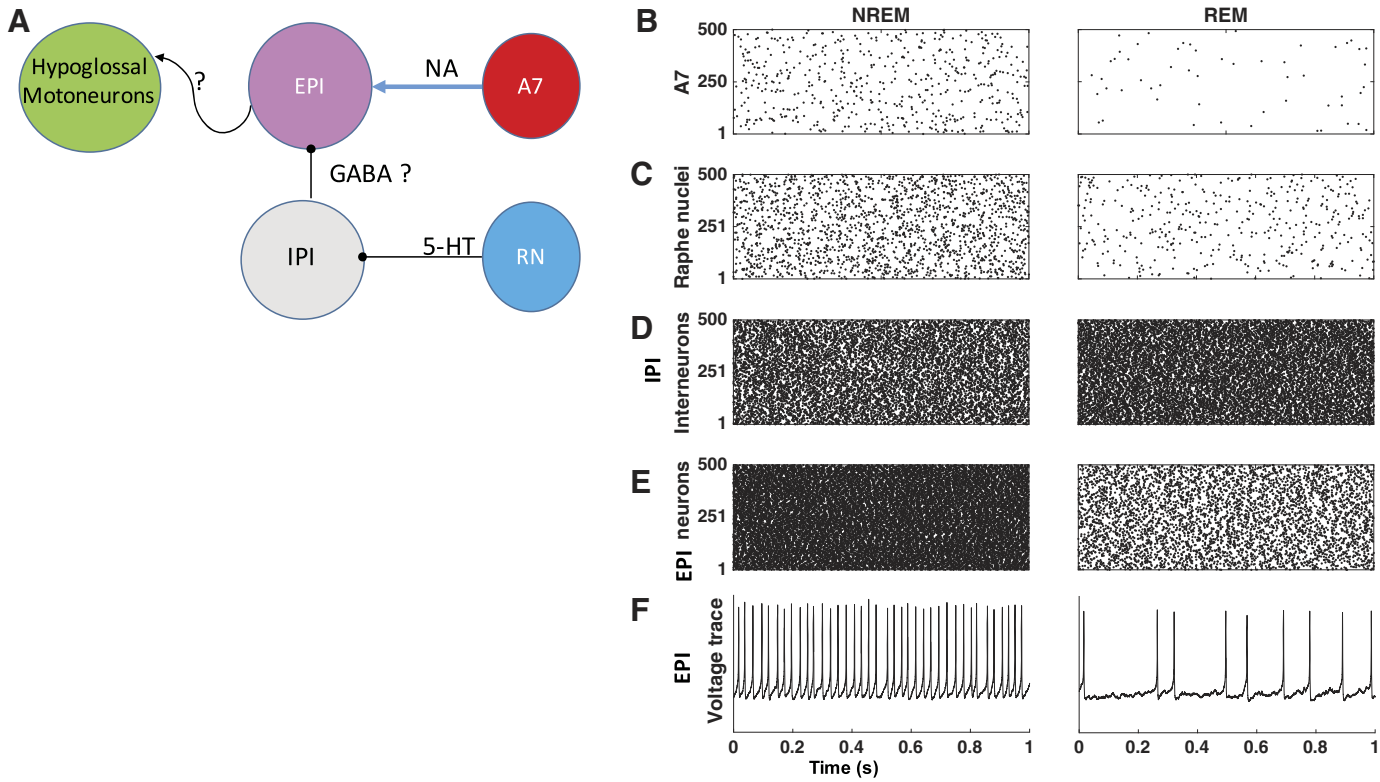

Fig. 2. Baseline model activity during rapid eye movement (REM) and non-REM (NREM) sleep. *A*: schematic of a biophysical model of brain-stem circuit. We assumed that raphe neurons (RN) inhibit inhibitory perihypoglossal interneurons (IPI) through 5-HT_{1A} receptors and IPI, in turn, inhibit excitatory perihypoglossal interneurons (EPI) by affecting $GABA_A$ receptors. EPI integrate both the excitatory noradrenergic drive from A7 noradrenergic (NA) nuclei and inhibitory drive from IPI. The neurotransmitter by which EPI population excites HMs has yet to be identified. *B* and *C*: raster plots show the A7 and RN firing during NREM and REM sleep. *D*: IPI are disinhibited during REM compared with NREM sleep. *E* and *F*: raster plots and voltage traces show higher activity of EPI during NREM compared with REM sleep.

the activity of IPI and EPI populations but not the firing rates of A7 or RN in our network model (Fig. 4, *C–F*). When the mixture of Pz and Me was applied, the EPI activity during NREM sleep was reduced to 24.59% of the baseline (the activity during NREM sleep under a drug-free condition). This level was similar to the level of the EPI activity during REM sleep in control (24.27% of the baseline). During the following REM sleep, the activity of EPI minimally decreased to 21.97% of baseline, which mimicked the experimentally observed abolition of REM-HD by Pz and Me.

In the prazosin only condition, the EPI activity reduced to 24.18% of baseline during NREM sleep and further reduced to 20.23% during REM sleep. This level of EPI activity was significantly ($P < 0.05$; $n = 500$; paired *t*-test) less compared with that during REM sleep after Pz and Me (21.97%), suggesting that Me has a disfacilitatory effect on EPI activity, which was also observed in in vivo experiments (Kodama et al. 2003). The estimated relative contribution of serotonergic mechanisms to REM-HD in the model was $(24.18 - 20.23)/(100 - 20.23) \approx 5\%$, and the relative contribution of norad-

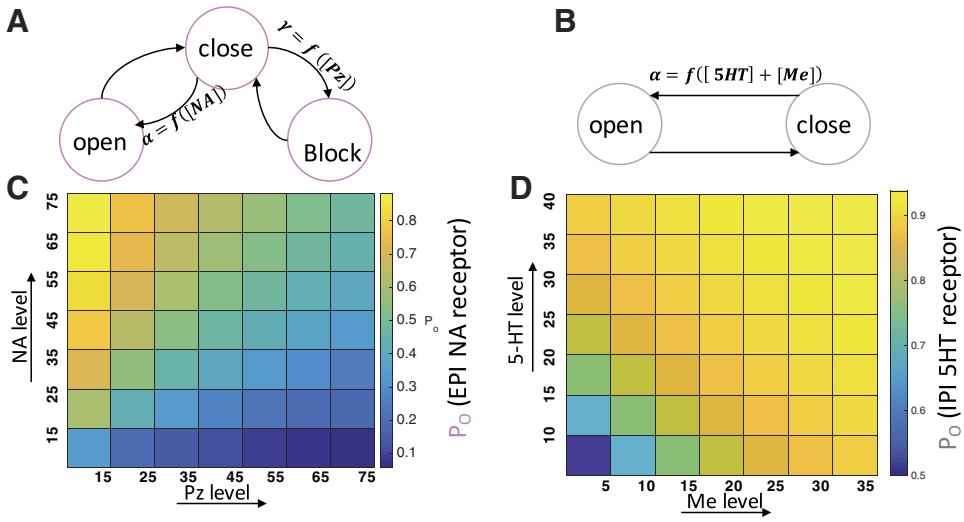

Fig. 3. The effect of different ligand concentrations on the state of α_1-adrenergic and 5-HT_{1A} receptors. *A*: dynamics of noradrenergic (NA) receptor under action of NA and prazosin (Pz) was modeled based on the transition between open, closed, and blocked states (see MATERIALS AND METHODS). $\alpha = K_4[NA]$, $\gamma = K_5[Pz]$. *B*: dynamics of 5-HT_{1A} receptor under the action of 5-HT and methysergide (Me) were modeled based on the transition between open and closed states. $\alpha = K_1([5\text{-HT}] + [Me])$. *C*: Pz competed with NA to reduce the probability of the NA receptor to be in the open state (P_O). *D*: Me helped 5-HT to increase the probability of the 5-HT_{1A} receptor to be in the open state. EPI, excitatory perihypoglossal interneurons; IPI, inhibitory perihypoglossal interneurons.

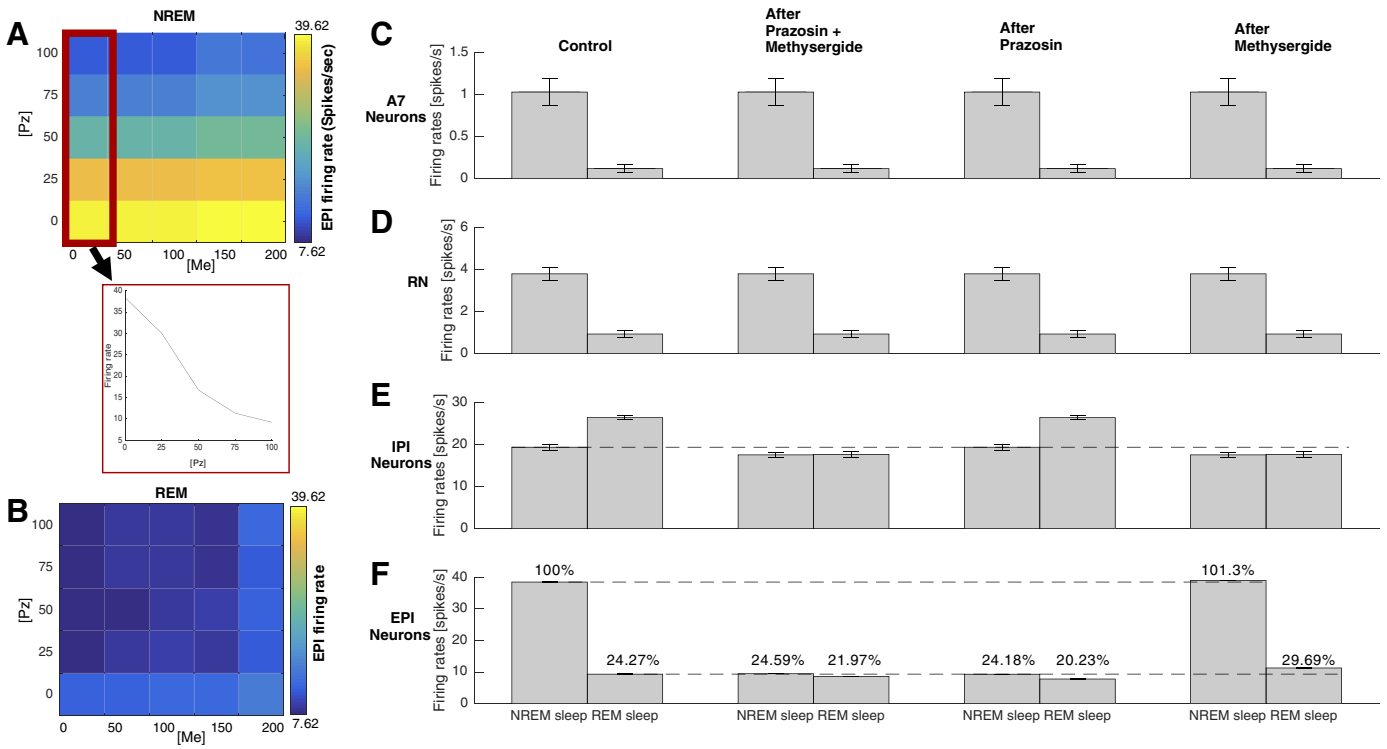

Fig. 4. Simulated effects of drug application in the model. *A*: effect of different levels of prazosin (Pz) and methysergide (Me) on the average firing rate of excitatory perihypoglossal interneurons (EPI) during non-rapid eye movement (NREM) sleep. *Inset* shows, for the minimum level of Me, that increasing the Pz level reduced the activity of EPI. *B*: effect of different levels of Pz and Me on the average firing rate of EPI during rapid eye movement (REM) sleep. *C* and *D*: average firing rates of A7 noradrenergic and raphe neurons (RN) during NREM and REM sleep, which were independent of the presence of either antagonist. *E*: inhibitory perihypoglossal interneurons (IPI) were disinhibited during REM sleep in control. The application of Me inhibited firing rate of IPI below the control NREM sleep level and made them state independent, i.e., insensitive to changes of the level of 5-HT. *F*: average firing rate of EPI during NREM and REM sleep under the drug-free control condition and after application of antagonists.

renergic mechanisms was 95%, which is consistent with the in vivo findings.

Under the methysergide only condition, the activity of IPI population was reduced during NREM sleep compared with baseline, which resulted in disinhibition of the EPI population to 101.3% of baseline (Fig. 4, *E* and *F*). During the following REM sleep, the activity of IPI population did not change because Me occupied all 5-HT_{1A} receptors, which made these neurons insensitive to state-dependent changes in 5-HT level (Fig. 4*E*). The activity of EPI group was largely depressed during REM sleep (Fig. 4*F*). However, it remained significantly higher than that during control REM sleep ($P < 0.05$; $n = 500$; paired *t*-test), mimicking the disinhibitory effect of methysergide on the REM-HD observed in vivo (see Fig. 1*C*).

In summary, the model explains the behavior of HMs that was observed in vivo. The only discrepancy was a little increase of activity of EPI that occurred during NREM sleep after application of Me, whereas in in vivo data, the activity of HMs was reduced during NREM sleep under the methysergide only condition (see Fig. 1*C*). The reason for this discrepancy can be explained by the fact that in our model we did not include the early direct effect of Me on HMs, which decreased activity of HMs immediately after Me injections but did not affect REM-HD in vivo (Fenik et al. 2005b). Taking this caveat into account, we concluded that the model confirms that serotonergic drive may be sufficient to explain disinhibition of HMs during REM sleep.

DISCUSSION

In vivo data suggest complex interaction between different types of neurotransmitters in the control of activity of HMs during sleep. Several brain-stem circuits are involved, and understanding of specific mechanisms is lacking, which limits developing novel therapeutic approaches. The respiratory-related activity of HMs has been modeled by inputs from Bötzinger, pre-Bötzinger, and caudal ventral respiratory group to understand the chemoreflex modulation of the respiratory and presympathetic networks (Barnett et al. 2017). However, the sleep-dependent activity of HMs under the influence of pharmacological agents has not been previously explained. The goal of this new study was to construct a biophysical model of the brain-stem neuronal network that may explain state-dependent activity of HMs and to test this model against in vivo data during the transitions from NREM to REM sleep and applications of noradrenergic and serotonergic antagonists either to support or refute the proposed hypothetical minimal network of modulation and control of HMs.

Excitatory and inhibitory perihypoglossal interneurons have been suggested to mediate state-dependent 5-HT and NA drives to HMs (Fenik 2015). Our network model included four distinct interacting neuronal groups: A7 noradrenergic neuron, serotonergic raphe neuron (RN), excitatory perihypoglossal interneuron (EPI), and inhibitory perihypoglossal interneuron (IPI) populations. In the model, REM-HD occurred when the A7 neurons and RN fired at their minimum rate. The behavior of EPI in the model corroborates that the state-dependent

control of HM excitability could be mediated by EPI that integrate both the excitatory noradrenergic drive from A7 nuclei and disinhibitory serotonergic drive from RN, which is mediated by IPI. By adjusting the drug-related parameters, the model was able to reproduce the responses to prazosin and methysergide during REM and NREM sleep. The model predicts that these changes may be explained by different transition kinetic schemes for α_1-adrenoceptors and 5-HT_{1A} receptors. By manipulating with the status of α_1-adrenoceptors in EPI and 5-HT_{1A} receptors in IPI groups in the model, we corroborated the hypotheses that *1*) noradrenergic disfacilitation and serotonergic disinhibition could provide a potential mechanism of monoaminergic contribution to REM-HD and *2*) the noradrenergic mechanisms could be the major contributor to hypoglossal depression during REM sleep-like state compared with the contribution of 5-HT mechanisms.

We constructed the model based on experimentally obtained results that combined injections of α_1-adrenergic and 5-HT receptor antagonists into the hypoglossal nucleus abolished REM-HD during carbachol-induced REM sleep-like state in anesthetized rats (Fenik et al. 2005b). The NA drive proved to be mostly responsible for REM-HD compared with 5-HT drive under those experimental conditions (Fenik 2015). These findings were confirmed by the Horner group (Chan et al. 2006) in chronically implanted behaving rats with recording of genioglossus (GG) muscle activity during natural REM sleep. The application of terazosin, an α_1-adrenoceptor antagonist, into the hypoglossal nucleus via a microdialysis probe significantly decreased REM-HD in respiratory-modulated activity of GG by ~50% compared with saline controls (Chan et al. 2006). This decrease of REM-HD was much smaller than the ~90% decrease of REM-HD that was observed in anesthetized rats after injections of prazosin (Fenik et al. 2005b, 2015), which may have at least two explanations. First, the concentration of terazosin that entered the hypoglossal nucleus from the microdialysis probe in this study (Chan et al. 2006) is unknown. Thus, following diffusion, its concentration at the vicinity of EPI could be insufficient to block all relevant α_1-receptors; therefore, only partial effect could be observed in that study. The dose-response experiments were not reported to see whether the effect of terazosin was saturated. In addition, we showed (see *inset* in Fig. 4*A*) that increasing Pz concentration in the model could reduce the activity of EPI. Therefore, it supports the suggestion that the smaller effect of terazosin could be related to the smaller drug concentrations. Second, the relatively small effect of terazosin may imply that, in behaving rats, additional neurotransmitter mechanisms may contribute to REM-HD during natural REM sleep, e.g., cholinergic inhibition (Grace et al. 2013). However, the magnitude of terazosin-induced decrease of REM-HD appeared to be the largest among the effects on REM-HD that were produced by the application of antagonists of glutamatergic (Steenland et al. 2006), serotonergic (Sood et al. 2005), GABAergic (Morrison et al. 2003), glycinergic (Morrison et al. 2003), or muscarinic receptors (Grace et al. 2013) using the same approach under the same experimental conditions.

In addition, phenylephrine, an α_1-adrenergic agonist, was applied in an attempt to rescue activity of HM during REM-HD in behaving rats (Chan et al. 2006). The application of phenylephrine increased respiratory-modulated GG muscle activity proportionally to that during control saline application in each behavioral state: wakefulness, NREM, and REM sleep. Thus there was no apparent change in REM-HD following the phenylephrine application, suggesting that the agonist could not reduce REM-HD in behaving animal. The failure of phenylephrine to rescue GG activity during REM sleep is readily explained by the following. Again, the amount of phenylephrine that leaves the probe and its actual concentration within the hypoglossal nucleus is unknown, but it can be assumed to be similar to that of terazosin (the concentration of both drugs was 1 mM in the probe; Chan et al. 2006). According to our experience, microinjections of phenylephrine into the hypoglossal nucleus in anesthetized rats produce relatively short-lasting responses (~15 min; Fenik et al. 1999) compared with the effect of prazosin, which lasted >3 h (Fenik et al. 2005b). This finding suggests that the removal of phenylephrine from extracellular fluid occurs at a larger rate than that of prazosin. Since the chemical formulae of prazosin and terazosin are almost identical, their pharmacokinetics are likely to be similar. Thus probably larger concentration of phenylephrine needs to be applied into the hypoglossal nucleus to reach EPI by diffusion. Based on this reasoning, it most likely that phenylephrine did not reach EPI in behaving rats where we believe it could rescue the activity of HMs during REM-HD. However, the moderate direct effect of phenylephrine on HMs in behaving rats is consistent with our experience in anesthetized rats (Fenik et al. 1999).

In the model proposed in this study, NA drive affects HMs indirectly, via EPI that have a net excitatory effect on HMs. The need for this group of interneurons was dictated by the fact that α_1-adrenergic and 5-HT receptor antagonists injected into HMs required 30–60 min to reach their target receptors in the carbachol model of REM sleep (Fenik et al. 2004, 2005a, 2005b). There are no definitive electrophysiological or anatomic data yet that would prove or disprove the proposed hypothetical circuit. However, recently, we (Fenik and Rukhadze 2016) obtained preliminary data that support the hypothesis that NA drive to HMs is not direct. In these experiments, we compared effects of large single injections of prazosin into the center of hypoglossal nucleus with the three prazosin injections, as described previously (Fenik et al. 2004, 2005a, 2005b), and concluded that the diffusion of antagonists to interneurons may be the only plausible explanation of the long latency of the antagonist effect observed in the original studies (Fenik et al. 2004, 2005a, 2005b).

The question of which neurotransmitter is used by EPI to excite HMs remains open. One possible candidate is glutamate, which is the most widely used excitatory neurotransmitter in the central nervous system. However, in experiments in chronically implanted behaving rats, effects of glutamate antagonists on REM-HD were unexpectedly weak (Steenland et al. 2006). Thus the neurotransmitters that are responsible for the net excitatory drive from EPI to HMs need to be identified in future studies.

We proposed that RN inhibit IPI through 5-HT_{1A} receptors and IPI, in turn, inhibit EPI by $GABA_A$ receptors. More experiments are needed to confirm that $GABA_A$ and 5-HT_{1A} receptors in the brain-stem circuit are involved in the state-dependent control of HM activity. Nevertheless, our model provides evidence that interneurons, such as EPI and IPI that mediate effects of A7 neurons and RN on HMs, may be necessary to explain the dynamics of HMs during different sleep stages and under different drug conditions. Indeed, a

simple model with direct inputs from A7 neurons and RN to HM fails to explain their complex behavior. We believe that the model proposed in our new study can be enriched with emerging data from in vivo experiments and can be used for further understanding the HMs dynamics in the normal and the pathological states.

To conclude, we developed a computational network model to investigate the impact of withdrawal of noradrenergic and serotonergic drives during NREM to REM sleep on HM activity. The model dynamics are consistent with a broad range of empirical data and make predictions about specific minimal circuit interactions that are sufficient to explain the observed in vivo phenomena. Although we cannot exclude that other neuronal circuits may be also involved, the results of our study predict the dynamics of the excitatory and inhibitory perihypoglossal interneurons during different sleep stages and under various pharmacological manipulations. These predictions can be tested in future in vivo studies. Importantly, our study suggests new targets for clinical interventions that may reduce severity of obstruction events in patients with OSA.

ACKNOWLEDGMENTS

Preprint is available at https://doi.org/10.1101/199117.

GRANTS

This work was supported by grants from the Office of Naval Research (Multidisciplinary University Initiative: N000141612829) and the National Heart, Lung, and Blood Institute (HL-116845, R01-HL-081823, R01-HL-085188, K24-HL-132105, and T32-HL-134632).

DISCLOSURES

No conflicts of interest, financial or otherwise, are declared by the authors. As an Officer of the American Thoracic Society, A. Malhotra has relinquished all outside personal income since 2012. ResMed provided a philanthropic donation to University of California, San Diego, in support of a sleep center.

AUTHOR CONTRIBUTIONS

I.R., V.B.F., and M.B. conceived and designed research; V.B.F. performed experiments; M.N., M.K., and G.P.K. analyzed data; A.M., F.L.P., I.R., and V.B.F. interpreted results of experiments; M.N. and V.B.F. prepared figures; M.N., M.K., A.M., and V.B.F. drafted manuscript; M.N., M.K., G.P.K., A.M., F.L.P., I.R., V.B.F., and M.B. edited and revised manuscript; M.N., M.K., G.P.K., A.M., F.L.P., I.R., V.B.F., and M.B. approved final version of manuscript.

ENDNOTE

At the request of the authors, readers are herein alerted to the fact that additional materials related to this manuscript may be found at the institutional Web site of the authors, which at the time of publication they indicate is: https://www.bazhlab.ucsd.edu/downloads/. These materials are not a part of this manuscript and have not undergone peer review by the American Physiological Society (APS). APS and the journal editors take no responsibility for these materials, for the Web site address, or for any links to or from it.

REFERENCES

Barnett WH, Abdala AP, Paton JF, Rybak IA, Zoccal DB, Molkov YI. Chemoreception and neuroplasticity in respiratory circuits. *Exp Neurol* 287: 153–164, 2017. doi:10.1016/j.expneurol.2016.05.036.

Bazhenov M, Timofeev I, Steriade M, Sejnowski TJ. Model of thalamocortical slow-wave sleep oscillations and transitions to activated states. *J Neurosci* 22: 8691–8704, 2002. doi:10.1523/JNEUROSCI.22-19-08691.2002.

Bellingham MC, Berger AJ. Presynaptic depression of excitatory synaptic inputs to rat hypoglossal motoneurons by muscarinic M2 receptors. *J Neurophysiol* 76: 3758–3770, 1996. doi:10.1152/jn.1996.76.6.3758.

Chan E, Steenland HW, Liu H, Horner RL. Endogenous excitatory drive modulating respiratory muscle activity across sleep-wake states. *Am J Respir Crit Care Med* 174: 1264–1273, 2006. doi:10.1164/rccm.200605-597OC.

Colbert CM, Pan E. Ion channel properties underlying axonal action potential initiation in pyramidal neurons. *Nat Neurosci* 5: 533–538, 2002. [Erratum in *Nat Neurosci* 5: 1017, 2002.] doi:10.1038/nn0602-857.

Colpaert FC, Niemegeers CJ, Janssen PA. In vivo evidence of partial agonist activity exerted by purported 5-hydroxytryptamine antagonists. *Eur J Pharmacol* 58: 505–509, 1979. doi:10.1016/0014-2999(79)90326-1.

Cressman JR Jr, Ullah G, Ziburkus J, Schiff SJ, Barreto E. The influence of sodium and potassium dynamics on excitability, seizures, and the stability of persistent states: I. Single neuron dynamics. *J Comput Neurosci* 26: 159–170, 2009. doi:10.1007/s10827-008-0132-4.

Destexhe A, Mainen ZF, Sejnowski TJ. An efficient method for computing synaptic conductances based on a kinetic model of receptor binding. *Neural Comput* 6: 14–18, 1994. doi:10.1162/neco.1994.6.1.14.

Destexhe A, Rudolph M, Fellous JM, Sejnowski TJ. Fluctuating synaptic conductances recreate in vivo-like activity in neocortical neurons. *Neuroscience* 107: 13–24, 2001. doi:10.1016/S0306-4522(01)00344-X.

Destexhe A, Rudolph M, Fellous JM, Sejnowski TJ. Kinetic models of synaptic transmission. In: *Methods in Neuronal Modeling*, edited by Koch C, Segev I. Cambridge, MA: MIT Press, 1998.

Eckert DJ, Malhotra A, Lo YL, White DP, Jordan AS. The influence of obstructive sleep apnea and gender on genioglossus activity during rapid eye movement sleep. *Chest* 135: 957–964, 2009. doi:10.1378/chest.08-2292.

Fenik V, Davies RO, Kubin L. Adrenergic receptor subtypes mediating excitatory effects in hypoglossal motoneurons (Conference Proceeding). *Sleep* 22, *Suppl* 1: S37, 1999.

Fenik V, Davies RO, Kubin L. Combined antagonism of aminergic excitatory and amino acid inhibitory receptors in the XII nucleus abolishes REM sleep-like depression of hypoglossal motoneuronal activity. *Arch Ital Biol* 142: 237–249, 2004.

Fenik VB. Revisiting antagonist effects in hypoglossal nucleus: brainstem circuit for the state-dependent control of hypoglossal motoneurons: a hypothesis. *Front Neurol* 6: 254, 2015. doi:10.3389/fneur.2015.00254.

Fenik VB, Davies RO, Kubin L. Noradrenergic, serotonergic and GABAergic antagonists injected together into the XII nucleus abolish the REM sleep-like depression of hypoglossal motoneuronal activity. *J Sleep Res* 14: 419–429, 2005a. doi:10.1111/j.1365-2869.2005.00461.x.

Fenik VB, Davies RO, Kubin L. REM sleep-like atonia of hypoglossal (XII) motoneurons is caused by loss of noradrenergic and serotonergic inputs. *Am J Respir Crit Care Med* 172: 1322–1330, 2005b. doi:10.1164/rccm.200412-1750OC.

Fenik VB, Fung SJ, Chase MH, Rukhadze I. Behavior of noradrenergic A7 neurons during sleep and wakefulness (Conference Proceeding). *Soc Neurosci Abstr A*. October 21, 2015, p. 815.21.

Fenik VB, Rukhadze I. Control of hypoglossal motoneuron excitability by noradrenergic neurons is not direct (Conference Proceeding). *Sleep (Basel)* 2016: A47, 2016.

Fleury Curado T, Fishbein K, Pho H, Brennick M, Dergacheva O, Sennes LU, Pham LV, Ladenheim EE, Spencer R, Mendelowitz D, Schwartz AR, Polotsky VY. Chemogenetic stimulation of the hypoglossal neurons improves upper airway patency. *Sci Rep* 7: 44392, 2017. doi:10.1038/srep44392.

Fung SJ, Chase MH. Postsynaptic inhibition of hypoglossal motoneurons produces atonia of the genioglossal muscle during rapid eye movement sleep. *Sleep* 38: 139–146, 2015. doi:10.5665/sleep.4340.

Grace KP, Hughes SW, Horner RL. Identification of the mechanism mediating genioglossus muscle suppression in REM sleep. *Am J Respir Crit Care Med* 187: 311–319, 2013. doi:10.1164/rccm.201209-1654OC.

Heym J, Steinfels GF, Jacobs BL. Activity of serotonin-containing neurons in the nucleus raphe pallidus of freely moving cats. *Brain Res* 251: 259–276, 1982. doi:10.1016/0006-8993(82)90743-0.

Horner RL, Shea SA, McIvor J, Guz A. Pharyngeal size and shape during wakefulness and sleep in patients with obstructive sleep apnoea. *Q J Med* 72: 719–735, 1989.

Horton GA, Fraigne JJ, Torontali ZA, Snow MB, Lapierre JL, Liu H, Montandon G, Peever JH, Horner RL. Activation of the hypoglossal to tongue musculature motor pathway by remote control. *Sci Rep* 7: 45860, 2017. doi:10.1038/srep45860.

Jordan AS, McSharry DG, Malhotra A. Adult obstructive sleep apnoea. *Lancet* 383: 736–747, 2014. doi:10.1016/S0140-6736(13)60734-5.

Kodama T, Lai YY, Siegel JM. Changes in inhibitory amino acid release linked to pontine-induced atonia: an in vivo microdialysis study. *J Neurosci* 23: 1548–1554, 2003. doi:10.1523/JNEUROSCI.23-04-01548.2003.

Komarov M, Bazhenov M. Linking dynamics of the inhibitory network to the input structure. *J Comput Neurosci* 41: 367–391, 2016. doi:10.1007/s10827-016-0622-8.

Krishnan GP, Filatov G, Shilnikov A, Bazhenov M. Electrogenic properties of the Na^+/K^+ ATPase control transitions between normal and pathological brain states. *J Neurophysiol* 113: 3356–3374, 2015. doi:10.1152/jn.00460.2014.

Kubin L, Kimura H, Tojima H, Davies RO, Pack AI. Suppression of hypoglossal motoneurons during the carbachol-induced atonia of REM sleep is not caused by fast synaptic inhibition. *Brain Res* 611: 300–312, 1993. doi:10.1016/0006-8993(93)90517-Q.

Kubin L, Tojima H, Davies RO, Pack AI. Serotonergic excitatory drive to hypoglossal motoneurons in the decerebrate cat. *Neurosci Lett* 139: 243–248, 1992. doi:10.1016/0304-3940(92)90563-M.

Lai YY, Kodama T, Siegel JM. Changes in monoamine release in the ventral horn and hypoglossal nucleus linked to pontine inhibition of muscle tone: an in vivo microdialysis study. *J Neurosci* 21: 7384–7391, 2001. doi:10.1523/JNEUROSCI.21-18-07384.2001.

Lydic R. The motor atonia of REM sleep: a critical topics forum. Introduction. *Sleep* 31: 1471–1472, 2008. doi:10.1093/sleep/31.11.1471.

Mainen ZF, Sejnowski TJ. Influence of dendritic structure on firing pattern in model neocortical neurons. *Nature* 382: 363–366, 1996. doi:10.1038/382363a0.

Malhotra A. Hypoglossal-nerve stimulation for obstructive sleep apnea. *N Engl J Med* 370: 170–171, 2014. doi:10.1056/NEJMe1314084.

Mezzanotte WS, Tangel DJ, White DP. Waking genioglossal electromyogram in sleep apnea patients versus normal controls (a neuromuscular compensatory mechanism). *J Clin Invest* 89: 1571–1579, 1992. doi:10.1172/JCI115751.

Morrison JL, Sood S, Liu H, Park E, Liu X, Nolan P, Horner RL. Role of inhibitory amino acids in control of hypoglossal motor outflow to genioglossus muscle in naturally sleeping rats. *J Physiol* 552: 975–991, 2003. doi:10.1113/jphysiol.2003.052357.

Parkis MA, Bayliss DA, Berger AJ. Actions of norepinephrine on rat hypoglossal motoneurons. *J Neurophysiol* 74: 1911–1919, 1995. doi:10.1152/jn.1995.74.5.1911.

Pillar G, Malhotra A, Fogel RB, Beauregard J, Slamowitz DI, Shea SA, White DP. Upper airway muscle responsiveness to rising P_{CO_2} during NREM sleep. *J Appl Physiol (1985)* 89: 1275–1282, 2000. doi:10.1152/jappl.2000.89.4.1275.

Purvis LK, Butera RJ. Ionic current model of a hypoglossal motoneuron. *J Neurophysiol* 93: 723–733, 2005. doi:10.1152/jn.00703.2004.

Remmers JE, deGroot WJ, Sauerland EK, Anch AM. Pathogenesis of upper airway occlusion during sleep. *J Appl Physiol Respir Environ Exerc Physiol* 44: 931–938, 1978. doi:10.1152/jappl.1978.44.6.931.

Rossier O, Abuin L, Fanelli F, Leonardi A, Cotecchia S. Inverse agonism and neutral antagonism at α_{1a}- and α_{1b}-adrenergic receptor subtypes. *Mol Pharmacol* 56: 858–866, 1999. doi:10.1124/mol.56.5.858.

Rukhadze I, Fenik VB, Branconi JL, Kubin L. Fos expression in pontomedullary catecholaminergic cells following rapid eye movement sleep-like episodes elicited by pontine carbachol in urethane-anesthetized rats. *Neuroscience* 152: 208–222, 2008. doi:10.1016/j.neuroscience.2007.11.013.

Sawczuk A, Powers RK, Binder MD. Spike frequency adaptation studied in hypoglossal motoneurons of the rat. *J Neurophysiol* 73: 1799–1810, 1995. doi:10.1152/jn.1995.73.5.1799.

Schwartz AR, Smith PL, Oliven A. Electrical stimulation of the hypoglossal nerve: a potential therapy. *J Appl Physiol (1985)* 116: 337–344, 2014. doi:10.1152/japplphysiol.00423.2013.

Scrogin KE, Johnson AK, Brooks VL. Methysergide delays the decompensatory responses to severe hemorrhage by activating 5-HT_{1A} receptors. *Am J Physiol Regul Integr Comp Physiol* 279: R1776–R1786, 2000. doi:10.1152/ajpregu.2000.279.5.R1776.

Sood S, Morrison JL, Liu H, Horner RL. Role of endogenous serotonin in modulating genioglossus muscle activity in awake and sleeping rats. *Am J Respir Crit Care Med* 172: 1338–1347, 2005. doi:10.1164/rccm.200502-258OC.

Steenland HW, Liu H, Sood S, Liu X, Horner RL. Respiratory activation of the genioglossus muscle involves both non-NMDA and NMDA glutamate receptors at the hypoglossal motor nucleus in vivo. *Neuroscience* 138: 1407–1424, 2006. doi:10.1016/j.neuroscience.2005.12.040.

Strollo PJ Jr, Soose RJ, Maurer JT, de Vries N, Cornelius J, Froymovich O, Hanson RD, Padhya TA, Steward DL, Gillespie MB, Woodson BT, Van de Heyning PH, Goetting MG, Vanderveken OM, Feldman N, Knaack L, Strohl KP; STAR Trial Group. Upper-airway stimulation for obstructive sleep apnea. *N Engl J Med* 370: 139–149, 2014. doi:10.1056/NEJMoa1308659.

Suratt PM, McTier RF, Wilhoit SC. Upper airway muscle activation is augmented in patients with obstructive sleep apnea compared with that in normal subjects. *Am Rev Respir Dis* 137: 889–894, 1988. doi:10.1164/ajrccm/137.4.889.

Traub RD. Simulation of intrinsic bursting in CA3 hippocampal neurons. *Neuroscience* 7: 1233–1242, 1982. doi:10.1016/0306-4522(82)91130-7.

Trinder J, Jordan AS, Nicholas CL. Discharge properties of upper airway motor units during wakefulness and sleep. *Prog Brain Res* 212: 59–75, 2014. doi:10.1016/B978-0-444-63488-7.00004-5.

Trulson ME, Jacobs BL. Raphe unit activity in freely moving cats: correlation with level of behavioral arousal. *Brain Res* 163: 135–150, 1979. doi:10.1016/0006-8993(79)90157-4.

Yamuy J, Fung SJ, Xi M, Morales FR, Chase MH. Hypoglossal motoneurons are postsynaptically inhibited during carbachol-induced rapid eye movement sleep. *Neuroscience* 94: 11–15, 1999. doi:10.1016/S0306-4522(99)00355-3.